HYDRODYNAMICS IN
HIGH-ENERGY NUCLEAR COLLISIONS

BY
MARKKU KATAJA

Academic Dissertation
for the Degree of
Doctor of Philosophy

Jyväskylä, Finland
May 1989

HYDRODYNAMICS IN
HIGH-ENERGY NUCLEAR COLLISIONS

BY
MARKKU KATAJA

Academic Dissertation
for the Degree of
Doctor of Philosophy

To be presented, by permission of the
Faculty of Mathematics and Natural Sciences
of the University of Jyväskylä,
for public examination in Auditorium S-212 of
the University of Jyväskylä on May 26, 1989,
at 12 o'clock noon

Jyväskylä, Finland
May 1989

Preface

This thesis is based on the work, which for my part has been carried out during the years 1985-1989 at the University of Jyväskylä and at the Massachusetts Institute of Technology. I wish to express my gratitude to these institutes for providing an excellent and encouraging working environment. I thank my colleagues and friends for many fruitful discussions and especially for creating the inspiring and free atmosphere which is a special character of these institutes.

I am greatly indebted to my collaborators Henrique von Gersdorff, Keijo Kajantie, Tetsuo Matsui, Larry McLerran and Vesa Ruuskanen, who made is possible for me to accomplish this thesis in the present form. Especially I want to thank my supervisor Vesa Ruuskanen for bringing me to this field of study and for his continuous and patient guidance throughout the work. I also want to thank Markku Lehto for careful and laborious reading of the manuscript and for many valuable suggestions.

Finally, I want to thank my wife Marjut for her unreserved support and patience, and my two little daughters Loviisa and Ritva-Liina, who ensured that I always had an alternative for working on this thesis.

Jyväskylä, May 1989
Markku Kataja

Abstract

This thesis is a review of six publications in which we make use of relativistic hydrodynamics to solve the evolution of matter produced in extremely energetic nucleus-nucleus collisions. In the first one of these papers we study the thermodynamics, the hydrodynamics and the decoupling conditions of such matter. We discuss the initial conditions for the flow, the hydrodynamic equations for the transverse expansion of matter assuming cylindrical symmetry and longitudinal boost invariance and finally present a numeric algorithm, which we use to integrate these equations. In the subsequent three papers this framework is utilized to calculate the transverse momentum spectra of hadrons, the dilepton production and the abundance of strange particles in the final state. The bag model equation of state is used to simulate the first-order phase transition between baryonless hadronic matter and quark-gluon plasma. In the fifth paper we include the particle production from decaying color electric field according to the flux tube model for heavy ion collisions. The hadronization is incorporated by introducing an equilibrium 'mixed state' of hadrons gas, plasma and the color field in analogy to the mixed phase described by the ordinary bag model equation of state. In the last paper I apply a 1+2 dimensional numeric code to analyze a 1+3 dimensional cylindrically symmetric flow of matter assumed to be formed in a central O+Pb collision at 200 GeV/nucleon. The flow data is used to calculate the pseudorapidity distribution of transverse energy for the produced pions.

List of contents

List of publications:

I   *Studies of the hydrodynamic evolution of matter produced in fluctuations in $p\bar{p}$ collisions and in ultra-relativistic nuclear collisions*, H. von Gersdorff, L. McLerran, M. Kataja and P. V. Ruuskanen, Phys. Rev. D**34**, 794 (1986).
https://doi.org/10.1103/PhysRevD.34.794

II   *Studies of the hydrodynamic evolution of matter produced in fluctuations in $p\bar{p}$ collisions and in ultra-relativistic nuclear collisions II. Transverse-momentum distributions*
M. Kataja, P. V. Ruuskanen, L. D. McLerran and H. von Gersdorff, Phys. Rev. D**34**, 2755 (1986).
https://doi.org/10.1103/PhysRevD.**34**.2755

III   *Transverse flow effects in dilepton emission*, K. Kajantie, M. Kataja, L. McLerran and P. V. Ruuskanen, Phys. Rev. D**34**, 811 (1986).
https://doi.org/10.1103/PhysRevD.**34**.811

IV   *Strangeness evolution in the central region of a heavy-ion collision with transverse flow effects*, K. Kajantie, M. Kataja, P. V. Ruuskanen, Phys. Lett. B**179**, 153 (1986).
https://doi.org/10.1016/0370-2693(86)90453-3

V   *Hadronization of the flux-tubes in ultrarelativistic nucleus-nucleus collisions*, M. Kataja, T. Matsui,
MIT preprint CTP# 1693 (1989), submitted to a special volume of Annals of Physics in honour of the seventienth birthday of Herman Feshbach.
https://doi.org/10.1016/0003-4916(89)90142-5

VI   *Three dimensional hydrodynamics of ultrarelativistic heavy ion collisions*
M. Kataja, Z. Phys. C**38**, 419 (1988).
https://doi.org/10.1007/BF01584390

1. Introduction

The far-reaching idea that protons, neutrons, pions and other hadrons might not be elementary particles themselves but, instead, be composite states of 'quarks', was put forward by Murray Gell-Mann in the early 1960's [1]. At present, it is generally believed that the hadrons actually consist of quarks and gluons, and that the dynamics of these particles is correctly described by Quantum Chromodynamics (QCD). In this non-Abelian gauge field theory, based on the group SU(3), the quarks appear in three different 'colors'. The strong interaction between colored particles is mediated by eight vector bosons, the gluons, which also carry color and can interact by exchanging other gluons. The experimental evidence supporting QCD and the predicted substructure of hadrons is now very compelling. The hierarchial structure of matter can thus be described by the sequence: matter consists of molecules, which consist of atoms, which consist of electrons and nuclei, and so on up to quarks and gluons (and leptons). A natural question then arises: in what manner is this new layer of the microscopic structure reflected in the macroscopic properties of matter? By compressing and/or heating atomic gas, it is possible to turn it into a plasma in which the electrons and the nuclei are free from their previous atomic bonds. Analogously, it is natural to assume that under suitable conditions matter could be turned into a new phase – the Quark-Gluon Plasma (QGP) [2], in which state quarks and gluons would not be confined inside nucleons anymore, but could travel freely within a larger plasma region. Indeed, using lattice QCD theory, it has been shown that such a transition really has to take place if hadronic matter can be heated up sufficiently [3]. From numeric lattice QCD calculations, it has been deduced that for baryonless matter the transition temperature is roughly 200 MeV [4]. For an ideal QGP consisting of massless quarks and gluons, this temperature would correspond to an energy density of few GeV/fm^3. There are only two situations in the Nature, where a large amount of QGP could possibly exist. The most remote one is the very early stage of the Universe shortly after the Big Bang, when the energy densities could have been high enough for QGP [5]. It has been speculated that relics from this era could still be left in the present Universe in the form of small QGP droplets [6]. Another possibility is provided by the late stages of heavy stars. When a large star

collapses, the matter density could finally become high enough so that a neutron star with a QGP core or an entire quark star could be formed [7].

From the characteristic temperature and density scales quoted above, it is clear that one can not produce truly macroscopic amounts of QGP artificially (the mass of one cubic centimeter of QGP would be of the order of 10^{12} kg). On the other hand, the energy density required for the transition is probably one order of magnitude, or perhaps just a few times, larger than the average energy density inside a nucleus. It seems possible that such an energy density could be transiently achieved in a collision of very energetic nuclei. Whether this is true, depends on how much the energy of the incoming nuclei is 'stopped' in the collision process. If the interactions between the nucleons inside the colliding nuclei are weak and few, the nuclei are very transparent to each other. In that case most of the available energy remains as kinetic energy of the nucleons; no high density region is formed. If, instead, numerous inelastic collisions take place as the nuclei penetrate each other, the nucleons are slowed down and plenty of secondary particles are created. High energy densities can then be achieved as a result of particle production and strong compression of nuclear matter: it might be possible to create and study QGP in laboratory conditions.

In addition to the required high energy density, the lifetime of the high-density state should also be long enough for thermalization and phase transition. Only then it is meaningful to talk about 'matter' or 'plasma' as a collective entity in the conventional sense of condensed matter physics. While the questions concerning the energy deposition, the thermalization and the possibility of phase transition strictly speaking still remain unanswered, several theoretical estimates [8, 9] and especially some recent experimental results do give rise to optimism. In Brookhaven National Laboratory oxygen and silicon nuclei have been accelerated up to the energy of 14 GeV/nucleon. In CERN the oxygen and sulphur projectiles with the maximum energy of 200 GeV/nucleon have been used. Fig. 1 (a) represents schematically a central O+Pb collision at CERN energies. In a simplified scenario, only ~ 50 nucleons in the central cylinder of the lead target will collide with the 16 nucleons of the oxygen projectile. In the collision, a dense and – as we hope – a thermalized 'hot tube' is formed, which consists of the incoming nucleons and

a large number of secondary particles. It is possible that some fraction of the hadronic matter in the hot tube is momentarily dissolved into QGP.

(a)

(b)
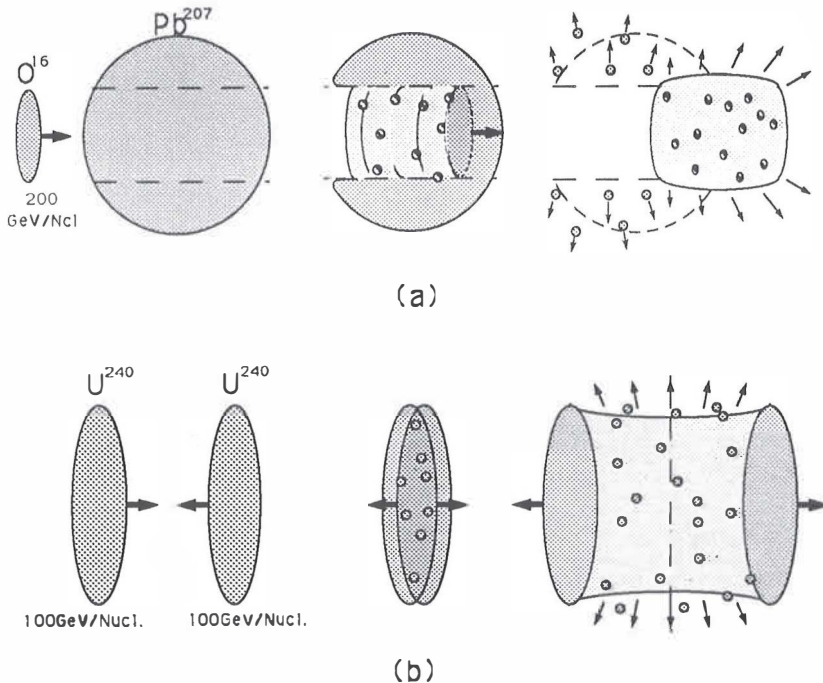
Fig. 1: A schematic illustration of a central O+Pb collision at CERN-SPS (a), and a central U+U collision at RHIC (b).

First data from the various experiments conducted at CERN and Brookhaven have recently been published [10, 11]. The results suggest that the achieved energy densities and the degree of thermalization are indeed high. Especially, the results from the pion interferometry seem to indicate a formation of a large, well thermalized, dense and relatively long living central region in oxygen induced reactions [12]. Some signals, like the J/Ψ suppression [10d], show a behavior, which could be explained by a formation of QGP – however, no firm conclusions can be drawn yet. What can be said is that these experiments do support the idea of using the heavy ion collisions as a tool to study the collective properties of extremely dense hadronic matter. It may be that the final judgement of the existence of QGP requires experiments with still higher energies.

The Relativistic Heavy Ion Collider (RHIC), which is planned to be built in Brookhaven, would provide uranium-uranium collisions with the energy of 100+100 GeV/nucleon (Fig. 1 (b)). At such energies the collision is in many respects simpler than the collision of two unequal nuclei at CERN. Firstly, it is expected that the original baryon number carried by the colliding nucleons is not strongly stopped. Thus, a central region is formed in which the matter consists of baryonless hadron gas or QGP. Secondly, it is expected that at these energies, the central region is approximately invariant under Lorentz-transformations in the longitudinal direction. This longitudinal boost invariance together with the cylindrical symmetry reduces the problem in the central region technically to 1+1 dimensions. Thirdly, the system is much bigger and the available energy is much larger than those achieved in the present accelerators. Keeping in mind the promising results from the present experiments, the prospects for obtaining and exploring QGP at RHIC can be considered good.

In order to extract information from the experimental particle distributions, a detailed description of the collision process is required. Two extreme approaches are possible: One can assume that a nucleus-nucleus collision is nothing but a sum of many nucleon-nucleon collisions. That is, there are no secondary collisions, no thermalization, no phase transition – altogether, no collective phenomena. With this assumption, one can predict the measurable quantities by a straightforward extrapolation from say, pp data. (At *very* high collision energy, thermalization and collective effects could be present already in hadronic collisions.) On the other extreme, one can assume that the mean free paths of particles become short quickly after the collision leading to a rapid thermalization. In that case, the evolution of the system can be described in terms of thermodynamics and hydrodynamics.

In this work, I present a series of studies $[I - VI]$, which take the latter approach assuming a complete local thermalization and which use relativistic hydrodynamics of ideal fluid to solve the evolution of matter created in the collision. The scenario applied throughout this work can be summarized as follows: The matter emerging from the primary collisions is assumed to be brought in local equilibrium at time τ_o after the collision. The state of the system at that time gives the inital condition for the hydrodynamic expansion, which is governed by the equation

$$\partial_\mu T^{\mu\nu} = 0. \qquad\qquad 1.1$$

For an ideal fluid the energy-momentum tensor $T^{\mu\nu}$ has the form

$$T^{\mu\nu} = (\varepsilon + p)u^\mu u^\nu - g^{\mu\nu}p, \qquad\qquad 1.2$$

where u^μ is the collective four-velocity of matter, ε and p are the local energy density and the pressure measured in the comoving frame of the fluid and $g^{\mu\nu}$ is the metric tensor. The equation 1.1 together with the definition 1.2 is merely an expression for the conservation of energy and momentum, and does not depend on the specific properties of the ideal fluid. The underlying microscopic dynamics is embedded in the equation of state, which gives relations between the thermodynamic quantities such as pressure, temperature, energy density, entropy density etc. and can include a phase transition. Given the initial conditions and the equation of state, one can solve the thermodynamic quantities and the flow velocity as a function of time and position. As the system expands and cools down, the mean free paths of the particles grow and finally exceed the characteristic size of the system. From that point on, hydrodynamics is not valid anymore: the fluid decouples into particles, which fly freely to detectors.

The used approach is conseptually simple and feasible. The numeric solution of the equations 1.1 enables one to calculate various measurable quantities such as the transverse momentum distribution of hadrons, the dilepton production and the abundance of strange particles. The numeric hydrodynamics has also been used as a basis of pion interferometric calculations [13]. The model has, however, some important limitations, which should be kept in mind when comparing with experiments. For example, it does not describe how the secondary particles are created and how they evolve prior to the thermalization. (An attempt is made in ref. [V] to resolve this deficiency in terms of the flux tube model in which the particles are created from a background color field.) Thus, even in the case that the produced matter would eventually be thermalized, some of the predicted signals lack the contributions from the primary collisions between the incident particles

and from the pre-thermalized matter. Furthermore, as a classical theory, the hydrodynamic model is deterministic: for a given initial condition and equation of state, the outcome is fixed (see, however [14]). Experimentally, the outcome from collisions with the same energy and impact parameter varies from event to event.

The standard prerequisites for the validity of ideal hydrodynamics are that the collision times and the mean free paths of particles should be much shorter than the expansion time and the characteristic size of the system, respectively. Rough estimates for the collision times and the mean free paths of various particle species range from about 0.1 fm to 2 fm at the energy density $\varepsilon = 1 - 10 \text{ GeV/fm}^3$ [I]. A reasonable and moderate assumption is that at these energy densities there is just one 'microscopic' (hadronic) scale of the order of 1 fm, which gives the collision time, the mean free path and the time scale associated with the phase transition process. This is to be compared with the 'macroscopic' scale, which is of the order of 10 fm and characterizes the expansion time and the size of the system. The difference between these microscopic and macroscopic scales is perhaps only one order of magnitude. The conditions for the ideal hydrodynamic flow may thus be at most marginally fulfilled. The non-equilibrium phenomena may be especially important at the early times and at the late times of the evolution. Furthermore, even in the case that the energy density momentarily exceeds the critical value for the phase transition, that stage might not live long enough for the phase transition to take place [15, 16]. In the hydrodynamic calculations presented here, we always assume that the phase transition is rapid and ignore possible supercooling and overheating effects.

The main part of this thesis consists of six publications $[I - VI]$, which were completed during the years 1986-1989. In ref. [I] we study the thermodynamics and the hydrodynamics of matter produced in the central region of extremely energetic heavy ion collisions. We discuss the initial conditions for the flow, write down the basic hydrodynamic equations for the transverse expansion of matter assuming cylindrical symmetry and longitudinal boost invariance and present the details of a computer code, which we use to integrate these equations. We also analyze the decoupling of matter, which takes place at a fixed low temperature T_{dec}. In ref. [II] we present numeric solutions for the hydrodynamic equations using the bag

model equation of state to simulate a first-order phase transition to QGP. The solutions are then used to calculate the transverse momentum distribution of hadrons and the dependence of the average transverse momentum on the total multiplicity. The latter quantity clearly reflects the properties of the equation of state. In refs. $[III]$ and $[IV]$ we use the solutions of ref. $[II]$ to calculate the dilepton and the strangeness production, respectively. The work reported in ref. $[V]$ is an attempt to extend the pure hydrodynamic model to incorporate secondary particle production by including an abelian color-electric field, which decays into particles by the Schwinger mechanism. The hadronization of the matter and the field is incorporated by introducing an intermediate mixed state between the plasma phase and the hadron phase in analogy to the mixed phase described by the ordinary bag equation of state. This leads to an extended bag equation of state in which the pressure and the temperature depend on the energy density of the particles and on the field strength. In ref. $[VI]$ a 1+2 dimensional numeric code is used to solve a 1+3 dimensional cylindrically symmetric flow of matter assumed to be formed in a central O+Pb collision at 200 GeV/nucleon (Fig. 1 (a)). The flow data is then used to calculate the pseudorapidity distribution of transverse energy for the produced pions.

In the following sections I review the main ideas and the conclusions of these works. Whenever possible, I attempt to assess the methods and the results from the point of view of more recent theoretical results, experimental data and common opinions. The second part of the thesis consists of the publications themselves.

2. Transverse flow in the central region of ultrarelativistic head-on nucleus-nucleus collisions

The principal goal of the work reported in refs. $[I - II]$ is to achieve a qualitative and to some extent a quantitative understanding of the evolution of matter expected to be produced in collisions of equal size nuclei at very high energies (RHIC). Among the topics are for example the time scales associated with the collision process: the thermalization time, the time spent in the different phases

of matter and the duration of evolution prior to decoupling. We discuss the initial conditions, the qualitative properties of the equation of state, the collective flow, the shock phenomena and the decoupling conditions. One purpose of this work is also to develop a practical computational framework to solve numerically the hydrodynamic equations for the transverse flow. The same numeric code is used later to estimate various measurable quantities.

According to numeric Monte Carlo simulations in lattice QCD, an abrupt change from hadronic gas with few degrees of freedom to QGP with a large number of degrees of freedom takes place at a narrow temperature range. There is still no consensus of the actual nature of this transition or of the exact value of the transition temperature T_c. The recent estimates for T_c seem to center around values slightly above 200 MeV [3]. The transition is qualitatively parametrized by the bag equation of state, which combines the equation of state of massless ideal pion gas at low temperatures with the equation of state of ideal QGP of massless quarks and gluons at high temperatures. It describes a first-order phase transition through a mixed phase in which the pion gas and QGP can coexist at a constant temperature T_c. The bag equation of state gives the pressure p in terms of the energy density ε as

$$p(\varepsilon) = \begin{cases} \frac{1}{3}\varepsilon, & \varepsilon < \varepsilon_H, & \text{(Hadron phase)}; \\ \frac{1}{3}\varepsilon_H, & \varepsilon_H < \varepsilon < \varepsilon_Q, & \text{(Mixed phase)}; \\ \frac{1}{3}(\varepsilon - 4B), & \varepsilon_Q < \varepsilon, & \text{(Plasma phase)}, \end{cases} \qquad 2.1$$

where

$$\begin{aligned} \varepsilon_H &= 3a_h T_c^4, \\ \varepsilon_Q &= 3a_q T_c^4 + B, \\ a_h &= 3\frac{\pi^2}{90} \approx 0.33, \\ a_q &= (2 \times 8 + \frac{7}{8} \times N_F \times 2 \times 2 \times 3)\frac{\pi^2}{90} \approx 4.62, \\ B &= T_c^4/(a_q - a_\pi) = \text{bag constant}, \\ N_F &= 2.5 = \text{number of quark flavors}. \end{aligned} \qquad 2.2$$

The value 2.5 for the number of quark flavors is chosen in order compensate for the fact that quark masses were neglected, i.e. to roughly take into account the fact that the heavier strange quark contributes less to the total pressure than the light up and down quarks.

We consider a central collision of two identical, strongly Lorentz-contracted nuclei as shown in Fig. 1 (b). The kinetic energy liberated in the primary collisions is materialized between the receding nuclei forming a longitudinally expanding cylinder. The original baryon number contained in the nuclei remains near the ends of the cylinder, which still move apart almost with the velocity of light. The longitudinal velocity of matter near the baryon-free central region is given by the scaling relation $v_z = z/t$ [9]. The assumed symmetries reduce the number of independent space-time variables to two, which we choose to be the proper time τ and the cylindrical radius r defined by

$$
\begin{aligned}
\tau &= \sqrt{t^2 - z^2}, \\
r &= \sqrt{x^2 + y^2}.
\end{aligned}
\qquad 2.3
$$

At proper time τ_o the matter is brought into local equilibrium at temperature T_o. The radial velocity of matter is taken to be zero at that time. By dimensional reasons, the inital time and the temperature can be argued to be related as $\tau_o T_o = \kappa$, where κ is an undetermined dimensionless constant of the order of 1. In our calculations, the value of κ has been fixed to 1.25 to give $\tau_o = 1$ fm when $T_o = 250$ MeV.

In the case of an isentropic and boost invariant expansion, the total entropy

$$
\frac{dS}{dy} = \pi R^2 \tau_o s_o \qquad 2.4
$$

in the central rapidity slab $-1/2 < \eta \equiv \mathrm{arth}(z/t) < 1/2$ is conserved. Here $R = 1.1 A^{1/3}$ fm is the radius of the colliding nuclei. The initial entropy density s_o has the value $4a_q T_o^3$ if $T_o > T_c$ and $4a_h T_o^3$ if $T_o < T_c$. Using the relation $(dS/dy) \approx 3.7 (dN/dy)$ between the entropy and multiplicity of massless pions, the

initial temperature in the central region can be written in terms of the normalized pion multiplicity $\mathcal{N} = (1/A^{2/3})(dN/dy)$ at $y = 0$ as

$$(T_o/\mathrm{GeV}) = \begin{cases} (\mathcal{N}/132.4a_h)^{1/2}, & \mathcal{N} < \mathcal{N}_H, & \text{(Hadron phase)}; \\ (T_c/\mathrm{GeV}), & \mathcal{N}_H < \mathcal{N} < \mathcal{N}_Q, & \text{(Mixed phase)}; \\ (\mathcal{N}/132.4a_q)^{1/2}, & \mathcal{N}_Q < \mathcal{N}, & \text{(Plasma phase)}, \end{cases} \qquad 2.5$$

where $\mathcal{N}_{H,Q} = 132.4a_{h,q}(T_c/\mathrm{GeV})^2$.

Using the variables 2.3 the hydrodynamic equations 1.1 reduce to two independent equations

$$\partial_\tau T^{00} = -\partial_r(T^{00}\tilde{v}_r) - (\frac{v_r}{r} + \frac{1}{\tau})(T^{00} + p),$$
$$\partial_\tau T^{01} = -\partial_r(T^{01}v_r) - \partial_r(p) - (\frac{v_r}{r} + \frac{1}{\tau})T^{01}, \qquad 2.6$$

where v_r is the radial flow velocity of matter and $\tilde{v}_r = (1 + (p/T^{00}))v_r$.

Solving the eqs. 2.6 numerically in the present case is a non-trivial technical task mainly for two reasons. Firstly, the system is exploding freely into vacuum. At the beginning of the expansion, matter is violently accelerated at the boundary, where the density and the pressure go sharply to zero. Later, a more extended region of diluted matter, moving almost with the velocity of light, is developed. For example the flow velocity of the fluid is calculated essentially as a ratio of the momentum and energy densities making it difficult to produce an accurate solution near the boundary, where these densities vanish. Secondly, when the bag equation of state is used, the transition from mixed to hadron phase can not take place continuously, but instead, through a shock front between the two phases [17]. The most frequently used methods for solving partial differential equations can not, as such, handle discontinuities, but must be supplemented by a suitable special treatment for shocks. Furthermore, in the present case, a shock can be formed spontaneously in an originally smooth solution at the point where $\varepsilon = \varepsilon_H$ (eq. 2.2). Thus, the method should also be capable of recognizing and determining the properties of a forming shock. This kind of approach has been developed and

succesfully used in refs. [18]. The SHASTA-FCT algorithm [19], which we use to integrate eqs. 2.6, was developed specifically for applications where discontinuities and sharp edges can occur. The idea of the FCT (Flux Corrected Transport) methods is to combine the best features of two different algorithms – a high-order and a low-order algorithm by giving the final result as a weighted sum of solutions produced by the two algorithms [20]. When the solution is smooth, the high order method is favored. Near steep gradients, however, the low-order method is used to an extent which is sufficient to prevent extensive dispersive errors, which are characteristic to high-order methods near sharp edges. In the SHASTA code, the proper weighting is performed automatically point by point – no special measures are needed to detect or treat shocks. In the present problem, this method has proven reliable and qualitatively accurate.

There is still another complication due to the appearance of shocks: In the case of free expansion into vacuum, there are no spatial boundary conditions. In that case, the solution at the discontinuity is not uniquely determined by the energy-momentum conservation only. The possible solutions are characterized by one additional parameter, which can be chosen to be the entropy production rate at the shock. In the SHASTA algorithm, this entropy production can be adjusted by weighting the low-order solution more than would be absolutely necessary to avoid too extensive dispersive errors. On the other hand, the low-order methods typically lead to numeric diffusion. In the SHASTA method this can be used to smooth the shock and to produce the entropy needed for a particular solution. Using the shock stability criteria, it can be argued that the most favorable solution is the Jouguet shock, which corresponds to the maximum entropy production for a given state of fluid into which the shock is propagating. We have verified that for a one dimensional shock, it is possible to produce the Jouguet shock by adjusting the parameter controlling the weight of the low-order solution in the SHASTA code.

A typical example of a flow pattern is shown in Fig. 2, where the contour curves for the energy density $\varepsilon(\tau, r)$ and for the radial velocity $v_r(\tau, r)$ are plotted for U+U collision using the initial temperature $T_o = 350$ MeV.
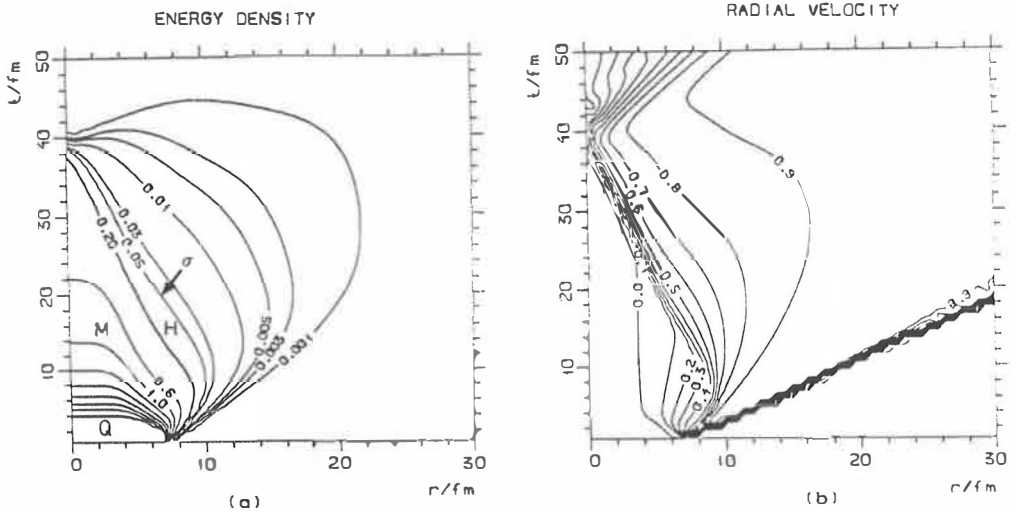
Fig. 2: Contour curves of constant energy density ε (GeV/fm^3) and radial velocity v_r for $T_o = 350$ MeV and $T_c = 200$ MeV. The plasma-mixed and mixed-hadron boundaries are indicated by the heavy contours $\varepsilon = \varepsilon_Q = 3.65$ and $\varepsilon = \varepsilon_H = 0.2$ in Fig. (a).

In the beginning, the hydrodynamic evolution is dominated by the fast cooling due to the longitudinal scaling expansion. The transverse flow is generated by pressure gradient at the edge of the cylinder leading to the rarefaction wave, which propagates into the plasma with the velocity of sound $c_s = 1/\sqrt{3}$. The edge of the matter shoots into the vacuum with the velocity of light. As the longitudinal expansion brings the energy density down to the upper critical value $\varepsilon_Q = 3.65$ GeV/fm^3 at the time $\tau_Q \approx 4$ fm, the interior of the cylinder turns into a mixed phase. In the mixed phase, the velocity of sound vanishes and the rarefaction wave is stopped, as can be seen from the velocity curves of Fig. 2 (b). The phase transition shock is developed on the outer edge of the mixed phase at $\varepsilon = \varepsilon_H = 0.2$ GeV/fm^3. It travels slowly inwards and reaches the center at the time $\tau_H \approx 40$ fm. By liberating latent heat associated with the first-order phase transition, the shock front effectively accelerates matter in transverse direction.

3. Decoupling and transverse momentum distributions

The flow data of Fig. 2 allows one to follow the motion and the temperature of a given fluid element as it evolves through the plasma and mixed phases and finally enters the hadron phase. As the matter still cools down, the mean free path of the pions in the element is increased until they can be expected to collide less than once in their future history: the fluid breaks into free particles. We do not take into account the possible entropy production, which could be present due to the large mean free path just prior to the decoupling, but assume that at a given temperature T_{dec}, the matter turns instantaneously from equilibrium pion gas to free particles. In the actual calculations we have used the value $T_{dec} = m_\pi \approx 140$ MeV, which corresponds to the energy density $\varepsilon_{dec} = 0.05$ GeV/fm^3 and defines the decoupling surface σ in Fig. 2 (a). The final distribution of pions is calculated as follows [21]: The number of pions in a phase space volume element $dV d^3p$, is given by

$$dN = \frac{g_\pi}{(2\pi)^3} f(p) dV d^3p, \qquad 3.1$$

where

$$f(p) = \frac{1}{e^{E/T_{dec}} - 1} \qquad 3.2$$

is the distribution function and $g_\pi = 3$ is the degeneracy of the pions. For a fluid moving with a four-velocity $u^\mu = \gamma(1, \vec{v}_r, z/t)$, we have to replace the volume element $dV d^3p$ and the pion energy E by the covariant forms $p^\mu d\sigma_\mu (d^3p/E)$ and $p^\mu u_\mu$, respectively. Integrating over σ, we obtain the invariant distribution

$$\frac{dN}{d^3p/E} = \frac{g_\pi}{(2\pi)^3} \int_\sigma f(p) p^\nu d\sigma_\nu. \qquad 3.3$$

The details of the hydrodynamic flow enter this integral through the four-velocity u^μ of the fluid and through the shape of the surface σ. Using the variables 2.3,

the r.h.s of equation 3.3 can be given explicitly in terms of the Bessel functions I_n and K_n as

$$
\frac{dN}{dydp_T^2} = \frac{g_\pi}{2\pi} \int_\sigma \tau r \sum_{n=1}^\infty \left[m_T I_0 \left(n \frac{p_T}{T_{dec}} \text{sh}(\alpha) \right) K_1 \left(n \frac{m_T}{T_{dec}} \text{ch}(\alpha) \right) dr \right.
$$
$$
\left. - p_T I_1 \left(n \frac{p_T}{T_{dec}} \text{sh}(\alpha) \right) K_0 \left(n \frac{m_T}{T_{dec}} \text{ch}(\alpha) \right) d\tau \right],
$$

3.4

where y is the rapidity, p_T is the transverse momentum and $m_T = \sqrt{m^2 + p_T^2}$ is the transverse mass of particles. The quantity $\alpha = \text{arth}(v_r)$ is the rapidity of the transverse flow. The p_T distributions of massless pions in U+U collisions for several multiplicities (initial temperatures) are shown in Fig. 3 [22].
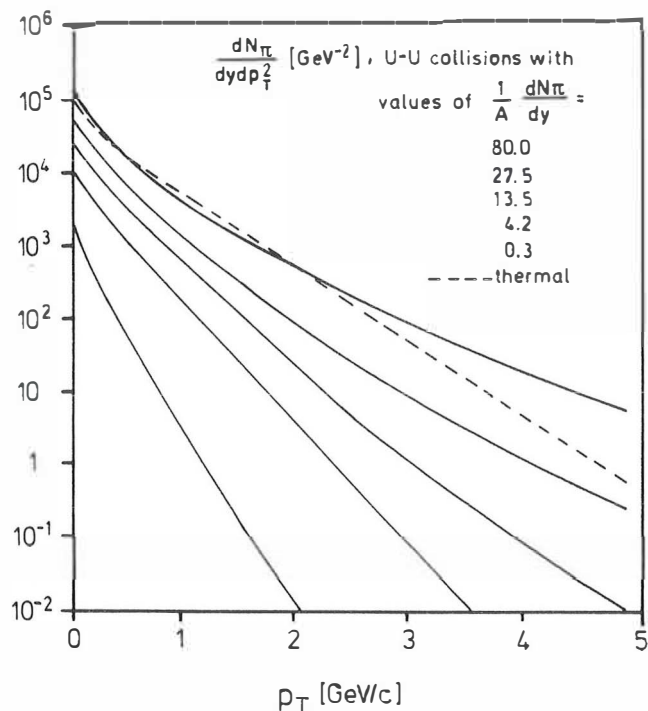
Fig. 3: Transverse momentum distributions of massless pions for various multiplicities in U+U collisions [22]. The dashed line is the thermal distribution with the same average p_T as in the case $(1/A)(dN/dy) = 80$.

For comparison, the thermal distribution (no flow) giving the same average p_T as the case $(1/A)dN/dy = 80$, is also shown. Unlike the thermal distribution, the curves obtained from the hydrodynamic calculation do not become exponential even at high values of p_T. This behavior can be traced back to the transverse flow at the decoupling [22]. For the flow illustrated in Fig. 2, $(1/A)dN/dy = 13.5$. In that case the enhanced tail of the p_T distribution comes from the times $\tau < 10$ fm, when the transverse velocity at the decoupling surface is high $(0.7 - 0.9)$. Instead, the steeper low-p_T part comes from later times when the transverse velocity on the decoupling surface is ~ 0.5 for a long period of time. Thus, in principle this behavior could be used to signal the presence of a collective transverse flow during the collision.

As one may note from eq. 2.5, in an adiabatic flow the total multiplicity dN/dy is a measure of the initial temperature T_o. On the other hand, if the transverse velocity vanishes initially, the average transverse momentum of the particles in the initial state is

$$\langle p_T \rangle \approx 2.12 \frac{[(1-r)g_\pi + r(g_g + \frac{7}{8}g_q)]}{[(1-r)g_\pi + r(g_g + \frac{3}{4}g_q)]} T_o, \qquad 3.5$$

where $g_{\pi,g,q}$ are the pion, gluon and quark degeneracy factors, respectively, and

$$r = \begin{cases} 0, & \mathcal{N} < \mathcal{N}_H, & \text{(Hadron phase)}; \\ (\mathcal{N} - \mathcal{N}_H)/(\mathcal{N}_Q - \mathcal{N}_H), & \mathcal{N}_H < \mathcal{N} < \mathcal{N}_Q, & \text{(Mixed phase)}; \\ 1, & \mathcal{N}_Q < \mathcal{N}, & \text{(Plasma phase)}, \end{cases} \qquad 3.6$$

where $\mathcal{N} = (1/A^{2/3})dN/dy$. For $\mathcal{N}_{H,Q}$, see eq. 2.5. In Fig. 4, the average transverse momentum of particles in the initial state has been plotted as a function of $(1/A^{2/3})dN/dy$ using the critical temperature $T_c = 200$ MeV.

According to eqs. 2.5 and 3.5, the transverse momentum rises as a function of multiplicity when the inital state is in the hadron phase, it stays almost constant over a large range of multiplicity corresponding to the initial state in the mixed phase and rises again in the plasma phase. It is interesting to see how this behavior
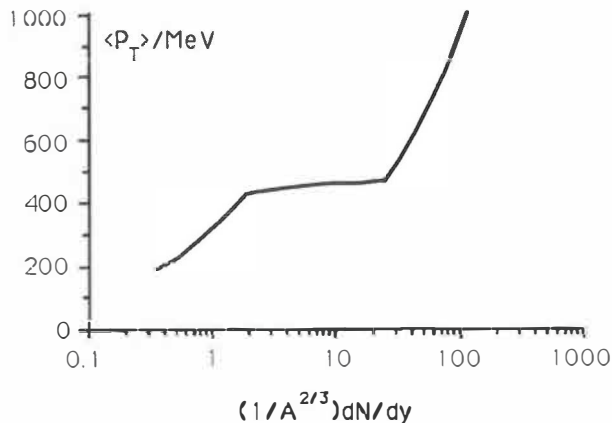
Fig. 4: The average transverse momentum of pions in the initial state as a function of multiplicity. (Eqs. 2.5, 3.5 and 3.6.)

is reflected in the average transverse momentum of the final-state pions. The hydrodynamic flow alters the initial $\langle p_T \rangle$ for several reasons. As discussed earlier, the transverse flow can be developed by pressure gradients in the hadron and plasma phases – leading to a rarefaction wave – or by converting latent heat into kinetic energy at the phase transition shock. Because the available latent heat, and thus the strength of the shock, increases with multiplicity within the mixed phase region, the average transverse momentum of final-state particles rises slowly through the mixed phase. When entering the plasma region, the shock has reached its maximum strength. In the plasma phase, however, a rarefaction wave can be formed. The higher the multiplicity (initial temperature), the more the rarefaction wave has time to develop and to gain strength in the plasma phase. This leads finally to a sharp rise in $\langle p_T \rangle$.

A remarkable feature seen in the numeric results is that the average transverse momentum plotted as a function of $(1/A)dN/dy$ is almost independent of the mass number A of the colliding nuclei (see Fig. 7 of ref. [II]). The actual scaling behavior of the transverse momentum and multiplicity are crucial on the experimental point of view. If $\langle p_T \rangle$ as a function of $(1/A)dN/dy$ does not depend on A and dN/dy scales as A, then, changing the size of the colliding nuclei would not help moving along the curve. This would make it difficult to probe the equation

of state by this method. As a matter of fact, the scaling in A is almost complete if $\langle p_T \rangle$ is plotted as a function of $(1/A^{5/6})dN/dy$, as shown in Fig. 5.
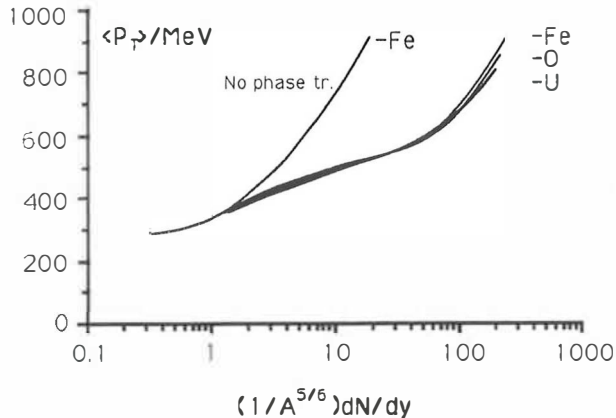
Fig. 5: The average transverse momentum of massless pions at decoupling as a function of $(1/A^{5/6})dN/dy$ for O+O, Fe+Fe and U+U collisions for $T_c = 200$ MeV. Also shown is the transverse momentum for Fe+Fe without phase transition ($T_c = \infty$).

Taking $A_{eff} = A_{projectile}^{2/3} A_{target}^{1/3}$, the average scaled multiplicity $(1/A_{eff}^{5/6}dN/dy)$ for the central O+Au collisions at 200 MeV/nucleon is ~ 7 [10b]. If dN/dy scales as $A^{4/3}$ (see e.g. [III]), the multiplicity $(1/A^{5/6}dN/dy)$ would be increased by a factor of ~ 2.5 when moving from O+Au to U+U collisions. If the fluctuations and the higher energy available at RHIC both introduce a factor of 2, one ends up with a maximum value of $(1/A^{5/6}dN/dy) \sim 70$ in RHIC U+U collisions. This may, or may not be high enough for observing the starting rise in the $\langle p_T \rangle$ curve, which would indicate the formation of the pure plasma phase. However, the flatness of the curve and perhaps even its decreasing slope in the mixed phase could be observed. Compare with the sharply rising curve in Fig. 5, which is calculated for Fe+Fe collisions using the equation of state for massless pion gas; $p = \varepsilon/3$. In fact, some hints of this kind of behavior have been seen in the photon spectrum by the CERN WA80 collaboration [10e].

Still another indication of the transverse flow could be achieved by comparing the

transverse momentum of different particle species. If the hydrodynamic evolution is dominated by light pions and if the heavier hadrons passively follow the flow, they are boosted to higher transverse momenta according to their masses. The $\langle p_T \rangle$ curves for kaons and nucleons should thus lie above that of pions as shown in Fig. 11 of ref. [II].

4. Dilepton production

The production of lepton pairs could in principle provide a clean probe for studying the various stages of the collision process. Once produced in the interior of the system, the leptons escape the high-density environment essentially without rescattering. They can be produced by the Drell-Yan mechanism in the hard primary collisions of nucleons, in the collisions between the secondary particles during the pre-equilibrium stage and in the thermalized matter during the hydrodynamic evolution. The Drell-Yan mechanism dominates the production of very massive pairs and is well known. The dilepton yield from the pre-equilibrium matter, instead, is difficult to estimate because of the poor knowledge of the equilibration processes. The production from the thermalized matter which, we hope, will dominate at least on some sufficiently large region of the total spectrum, can be calculated using the flow data provided by hydrodynamics. The thermal emission rate of lepton pairs from the processes $q\bar{q} \to ll$ in the plasma phase is given by

$$\frac{dN}{dM^2 d^3p/E} = \frac{\alpha}{8\pi^4} \sum_q e_q^2 \int_Q d^4x \, e^{\frac{-u\cdot p}{T}}, \qquad 4.1$$

where p^μ is the momentum and $M^2 = p^2$ is the invariant mass squared of the lepton pair and u^μ is the four-velocity of the fluid. The integration is performed over the four-volume occupied by the pure plasma. The emission rate from the hadron phase is given by

$$p^o \frac{dN}{dM^2 d^3p} = \frac{\alpha}{8\pi^4} G(M^2) \int_H d^4x \, e^{\frac{-u\cdot p}{T}}, \qquad 4.2$$

where

$$G(M^2) = \left(1 - \frac{4m_\pi^2}{M^2}\right) \frac{1}{12} F^2(M^2). \qquad 4.3$$

Here F is the form factor for the process $(\pi\pi \to ll)$. Including only the ρ pole, it takes the form

$$F^2(M^2) = \frac{m_\rho^4}{(m_\rho^2 - M^2)^2 - m_\rho^2 \Gamma_\rho^2}, \qquad 4.4$$

where the width of the ρ resonance $\Gamma_\rho = 0.155$ GeV and the mass $m_\rho = 0.77$ GeV. Here the contributions from other resonances like Ψ and ϕ have been neglected as well as the brehmsstrahlung, which dominates the production of pairs with very small masses. The total yield from the mixed phase is the averaged sum of 4.1 and 4.2 with the weighting given locally by the relative volumes occupied by each phase in the mixture.

In Fig. 6, the calculated dilepton spectrum from the pure plasma phase and from the hadron and mixed phases is illustrated qualitatively as a function of the pair mass M and the transverse momentum p_T. The effect of the transverse expansion is demonstrated by comparing the results (a), without and (b), with the transverse flow.

Unless the initial temperature is very high, the transverse flow has little time to develop in the plasma phase before the longitudinal cooling turns it into a mixed phase and the propagation of the rarefaction wave is stopped. Consequently, the dilepton spectrum from the plasma phase (Q) is not significantly affected by the transverse flow. The flat plasma contribution decreases slowly (in a logarithmic scale) with increasing M and p_T. (For quantitative behavior, see Figs. 6 – 9 of ref. [III]). The hadron+mixed contribution (H+M), instead, is characterized by the ρ peak and depends strongly on the transverse flow. Without transverse expansion, the H+M contribution dominates the low p_T spectrum but decreases steeply with increasing p_T. Thus, the ρ peak dissappears below the plasma contribution in Fig. 6 (a). With moderate initial temperatures, the transverse expansion affects
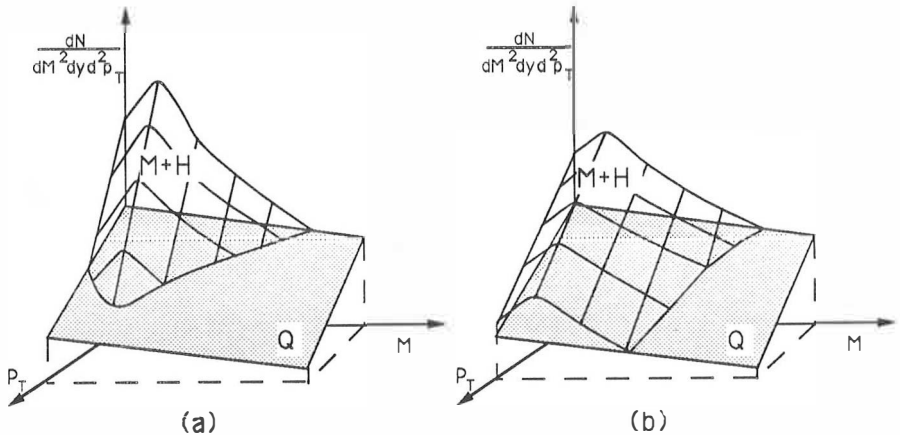
Fig. 6: A qualitative illustration of the dilepton emission from the plasma phase
(Q), and from the mixed and hadron phases (M+H) as a function of the
invariant mass M and the transverse momentum p_T of a lepton pair. Fig.
(a) is for the longitudinal expansion only. Fig. (b) includes the effects of
the transverse flow.

significantly only the mixed and hadron phases. The lepton pairs produced in
these phases then acquire additional transverse momentum from the flow. This
leads to a broadening of the M+H contribution in the p_T direction. The effect is
sufficiently strong to keep the ρ peak above the flat plasma contribution, or even
to increase its relative magnitude. The persistence of the ρ peak up to high values
of p_T (4 GeV, say) could thus indicate the existence of transverse flow.

As noted above, the low-mass pairs are dominantly emitted from the mixed and
hadron phases, while the pairs with medium and high masses come from the plasma
phase and possibly from the pre-equilibrium matter. The Drell-Yan emission dom-
inates the production of pairs with very high masses. If the multiplicity of an event
is high enough, a window in M could exist, which is dominated by the emission
from plasma. This part of the spectrum is sensitive to the initial conditions set by
τ_o and T_o and could be used to measure these parameters. If entropy is conserved
during the expansion, the total multiplicity dN/dy fixes the number $\tau_o T_o^3$. For
example, the pairs ($\tau_o = 0.5$ fm, $T_o = 500$ MeV) and ($\tau_o = 1.5$ fm, $T_o = 350$ MeV)

both correspond to the same multiplicity. If the expansion started at $\tau_o = 0.5$ fm with $T_o = 500$ MeV, the longitudinal expansion would cool the matter down to $T = 350$ MeV by the time $\tau = 1.5$ fm. The transverse flow developed during this time is not significant. Thus, the hydrodynamic flow after the time $\tau = 1.5$ fm, and consequently, the pion spectra are almost identical for these two cases. The degeneracy is resolved by the high-mass dilepton production, which differs considerably for the two cases – perhaps a factor of 2-3 at $M = 2$ GeV and factor of 4-5 at $M = 3$ GeV [22]. This is simply because of the fast production of high-mass lepton pairs during the time 0.5-1.5 fm in the case ($\tau_o = 0.5$ fm,$T_o = 500$ MeV), which is missing in the other case. In practice, however, this signal may be obscured by the Drell-Yan and pre-equilibrium productions.

5. Strangeness production

In hadronic collisions with energies above 10 GeV the relative abundance of strange particles is ~ 0.05 [23, 24]. For an equilibrium plasma with three flavors of quarks (u, d, s), the ratio of the number of s quarks to all particles is ~ 0.11, which value depends only weakly on the temperature. Due to the fast process $gg \leftrightarrow s\bar{s}$, the abundance of strange quarks could evolve close to this equilibrium value during the short lifetime of the plasma [25]. For the hadron gas of massless pions and kaons with mass $m_K = 0.5$ GeV, the ratio of K^-'s and $\bar{K}^o$'s to all particles is ~ 0.12 at $T = 140$ MeV and ~ 0.21 at $T = 240$ MeV according to the Maxwell-Boltzmann statistics. However, at the temperatures which are low compared to the kaon mass ~ 500 MeV the strangeness changing hadronic processes are suppressed. An enhanced abundance of strangeness in nuclear collisions could thus indicate a formation of plasma or a hot and/or long-living thermalized hadron gas.

In ref. $[IV]$ we have applied the cylindrically symmetric and boost invariant hydrodynamics to calculate the strangeness production at the central region. The local density of strange particles is $n = (1 - h)n_s + hn_{K^- + \bar{K}^o}$, where h is the relative volume occupied by the hadron gas (h is 0 in the plasma phase and 1 in the hadron phase). Here, n_s is the density of the strange quarks and $n_{K^- + \bar{K}^o}$ is

that of the strange hadrons. The initial condition for n is set in the plasma phase by $n(\tau = \tau_o) = n_s^{eq} \approx (T_o/200\,\text{MeV})^3(1/\text{fm}^3)$. During the hydrodynamic expansion, the strange particles passively follow the flow determined by the equations (2.6). The density n thus evolves according to the continuity equation

$$\partial_\mu(nu^\mu) = R_{gain} - R_{loss}, \qquad\qquad 5.1$$

where the four-velocity of the flow u^μ is solved from the eqs. 2.5. In the mixed phase we need an additional equation,

$$u^\mu\partial_\mu n_s = (R_{gain} - R_{loss})_Q, \qquad\qquad 5.2$$

which together with 5.1 gives the rate of conversion of strangeness from quark degrees of freedom to hadrons during the phase transition. The rate terms on the right-hand side of eq. 5.1 take into account the processes $gg \leftrightarrow s\bar{s}$ and $q\bar{q} \leftrightarrow s\bar{s}$ in the plasma phase and $K\bar{K} \leftrightarrow n\pi$ in the hadron phase. In eq. 5.2 only the plasma contribution is included. We use the explicit rate terms given in ref. [26], but vary the poorly known total cross section for the strangeness changing processes in the hadron phase in the range 2-20 mb.

The relative number of K^-'s and $\bar{K}^o$'s to all particles in the final state is calculated by integrating the kaon and total particle number fluxes over the decoupling surface σ:

$$\frac{dN_{(K^-+\bar{K}^o)}/dy}{dN_{tot}/dy} = \frac{\int_\sigma n_{(K^-+\bar{K}^o)}u^\mu d\sigma_\mu}{\int_\sigma n_{tot}u^\mu d\sigma_\mu}. \qquad\qquad 5.3$$

This ratio does not depend significantly on the decoupling temperature because the strangeness content effectively freezes out when the matter enters the hadron phase. If the rate of the hadronic processes is fast enough, the kaon content could be brought close to its equilibrium value during the relatively long-living mixed phase. If instead, hadronic processes are very slow compared to the lifetime of the mixed phase, the final abundance of strangeness reflects the equilibrium value in the plasma phase. According to our numeric results using $T_c = 200$ MeV, the

values of the ratio 5.3 range from 0.11 to 0.15 depending on the cross section for the hadronic processes.

It should be emphasized, that the rate terms in eqs. 5.1-5.2 do not take into account strangeness production due to the phase transition itself [23]. In order to preserve or increase entropy in the phase transition, where quarks and gluons are combined to hadrons, quark-antiquark and gluon pairs must be created. In spite of the larger mass of the strange quarks, a considerable number of them can be created in the process. This effect has been evaluated in later works and found to be very important [23, 27].

The enhanced abundance of strangeness in nuclear collisions could occure due to several mechanisms including a purely hadronic scenario. In order to make a distinction between the different possibilities, a very good knowledge of the strangeness changing processes is required. However, according to all the scenarios quoted here, the enhanced abundance of strangeness does imply that high densities and collective phenomena have occured during the collision.

6. Flux-Tube model, particle production and hadronization

In hydrodynamic models the evolution of the averaged local quantities such as temperature, flow velocity etc. is described by a compact set of hydrodynamic equations and by the equation of state which involves the properties of matter. In the previous sections $[I - IV]$ the hydrodynamic approach was applied to study the transverse expansion of matter produced in a central nucleus-nucleus collision assuming cylindrical symmetry and longitudinal boost invariance. The bag model equation of state was utilized to simulate a first-order phase transition. In this approach the transition from the unconfined plasma phase to the confined hadron phase takes place via an equilibrium mixed state in which the two phases coexist as a homogeneous mixture at a constant temperature and pressure. The numeric solution of the hydrodynamic equations was then used to calculate various measurable quantities such as the transverse momentum distributions and the dilepton and strangeness production at the central rapidity region.

The final results extracted from the model tend to be quite sensitive to the assumed equation of state and the initial condition, which both are beyond the scope of the hydrodynamic model itself. The 'initial condition' was given at some finite time τ_o after the collision. The initial temperature T_o was a free parameter, although an argument was given to relate τ_o and T_o. As such, the model makes no effort in describing how the initial kinetic energy was deposited into the central region and refrains from describing the period of time from the collision to τ_o.

The energy deposition and particle formation in the central region is naturally involved in the recent flux tube model for ultrarelativistic heavy ion collisions [28, 29]. In this model, the Lorentz-contracted nuclei are assumed to become color charged by a random color exchange between the colliding nucleons [30]. A strong color-electric field – the 'giant flux tube' – exerted between the receding nuclei polarizes the vacuum creating quark and gluon pairs through the Schwinger mechanism [31]. The subsequent evolution of the matter and the abelian color field are described by the relativistic Boltzmann-Vlasov and Maxwell's equations. In ref. [29] the transverse expansion of the plasma and the field was solved on the hydrodynamic limit ('electrohydrodynamics') using a geometrical set-up similar to that in the hydrodynamic calculations of refs. $[I - IV]$. While the model succesfully describes the formation of matter as unconfined plasma, it lacks a description of color confinement and hadronization. As such, it can only be adequate for the very early times of evolution and its predictive power is limited.

Having noticed the somewhat complementary properties of the two models outlined above, an apparent question arises: could it be possible to introduce a confinement and hadronization scheme into the electrohydrodynamic flux-tube model in analogy to the one used in the hydrodynamic calculations? The transition from plasma to hadrons would then take place in the bulk of matter through consecutive equilibrium states, which could be described by an 'equation of state' involving both the local thermodynamic and the field variables. In ref. $[V]$ we find an example of such an extended equation of state by generalizing the bag model equation of state to accommodate the abelian color-electric field. As a starting point and motivation, we use two ideas which in effect lead to a confinement of particles and fields in classical bag models: the fundamental bag pressure and the field-

dependent color-dielectric constant which vanishes in the real vacuum of QCD
[32]. The latter assumption is the basis of classical flux-tube models. It leads to
an effective confinement of the abelian color-electric field simply because the elec-
trostatic energy of the field outside the bag would be infinite (see e.g. [33]). The
generalized bag equation of state is derived below by considering an equilibrium
'mixed state', which is formed as the original giant flux tube is fragmented into
many smaller tubes, which are surrounded by hadron gas.

6.1 Mixed state of hadrons, plasma and color field

Consider a strong color-electric field spanned between large, parallel, charged ca-
pacitor plates. Through the Schwinger mechanism the field creates particles by
vacuum polarization. Originally, the created matter must be in the form of quarks
and gluons. The pair production gives rise to a polarization current, which to-
gether with a possible conduction current begins to neutralize the charges on the
capacitor plates and thus to reduce the total flux of the field. Assume, that un-
der suitable conditions, a 'mixed state' can be formed in which the field and the
plasma are confined into tubelike regions between the capacitor plates and the
space between the tubes is filled by hadron gas (Fig. 7).

In the simplest case, which we consider here, the matter between the tubes is ideal
gas of massless pions and the plasma consists of ideal gas of massless quarks and
qluons with zero net baryon number. The perturbative vacuum inside the tubes
is associated with a constant energy density $\mathcal{B}$ (the bag constant).

Consider a sample volume element ΔV near the central plane between the ca-
pacitor plates (Fig. 7). We assume that the matter is in thermal equilibrium
at temperature T and that the longitudinal color-electric field has a constant
strength $\mathcal{E}$ inside the tubes within ΔV. In mechanical equilibrium the pressure
$p_h = a_h T^4$ of the hadron gas between the tubes is equal to the total transverse
pressure $p_p = a_q T^4 + \frac{1}{2}\mathcal{E}^2 - \mathcal{B}$ inside the tubes. An equilibrium between the tubes
and the hadron gas is possible if $\mathcal{E} \leq \sqrt{2\mathcal{B}}$. The pressure balance then gives the
field-dependent transition temperature $T_c(\mathcal{E})$ as

Fig. 7: A schematic illustration of the mixed state of pion gas, quark-gluon plasma and the abelian color-electric field.

$$T_c^4(\mathcal{E}) = T_{co}^4 \left(1 - \frac{\mathcal{E}^2}{2\mathcal{B}}\right), \qquad\qquad 6.1$$

where T_{co} is the transition temperature in the absence of the field (the usual transition temperature of the ordinary bag equation of state). The transition temperature is thus lowered by the field, which is in accordance with the intuitive expectation that inside the tube the field acts in concert with the thermal motion to prevent particles from forming bound states.

Let ΔV_p be the total volume occupied by the tubes in ΔV and define the ratio

$$r = \Delta V_p / \Delta V. \qquad\qquad 6.2$$

The total energy density, averaged over ΔV, is given by $\varepsilon = (1-r)\varepsilon_h + r\varepsilon_p$, where $\varepsilon_h = 3a_h T^4$ and $\varepsilon_p = 3a_q T^4 + \frac{1}{2}\mathcal{E}^2 + \mathcal{B}$. The average entropy density s and the pressure p are defined analogously (in the mixed state, $p = p_h(\mathcal{E}) = p_p(\mathcal{E})$).

Note that because the field strength vanishes outside the tubes, the average field strength $\mathcal{D}$ is just $r\mathcal{E}$. The basic thermodynamic relations for these averaged variables are

$$
\begin{aligned}
\varepsilon + p &= Ts + \mathcal{E}\mathcal{D}, \\
\mathcal{D} &= r\mathcal{E}, \\
d\varepsilon &= Tds + \mathcal{E}d\mathcal{D}, \\
dp &= sdT + \mathcal{D}d\mathcal{E},
\end{aligned}
\qquad 6.3
$$

which hold for all three possible states of the system: in the hadron phase $r = 0$, $T < T_c$; in the mixed state $0 < r < 1$, $T = T_c(\mathcal{E})$ and in the plasma phase $r = 1$, $T > T_c$. Interpreting r as a 'dielectric constant' and $\mathcal{D}$ as an 'electric displacement', the eqs. 6.3 are formally the thermodynamic relations of the ordinary dielectric medium [34] – the relation $\mathcal{D} = r\mathcal{E}$ is the 'constitutive equation'. We note that in the classical dielectric models of confinement, bag model corresponds to the choice that the dielectric constant $\epsilon(\mathcal{E})$ is 0 below and 1 above some critical field strength $\mathcal{E}_o$, which defines the bag boundary [33]. If one takes the dielectric constant here to be 0 outside and 1 inside the tubes, the volume ratio r is just the average dielectric constant.

In the next section, we derive the hydrodynamic and field equations for the averaged quantities in the mixed state. To be able to solve these equations in practice, we must express p and r in terms of, say, ε and $\mathcal{D}$. For practical reasons it is, however, more favorable to use first $\mathcal{E}$ instead of $\mathcal{D}$ and then convert to $\mathcal{D}$ using the equation $\mathcal{D} = r(\varepsilon, \mathcal{E})\mathcal{E}$. We first define the $\mathcal{E}$ dependent lower and upper transition energy densities ε_H and ε_P by

$$
\begin{aligned}
\varepsilon_H(\mathcal{E}) &= \varepsilon_h(\mathcal{E}, T_c) = \varepsilon_H^o(1 - \frac{\mathcal{E}^2}{2\mathcal{B}}), \\
\varepsilon_P(\mathcal{E}) &= \varepsilon_p(\mathcal{E}, T_c) = \varepsilon_Q^o(1 - \frac{\mathcal{E}^2}{2\mathcal{B}}) + \mathcal{E}^2,
\end{aligned}
\qquad 6.4
$$

where $\varepsilon_H^o = 3a_h T_{co}^4$ and $\varepsilon_Q^o = 3a_q T_{co}^4 + \mathcal{B} = \varepsilon_H^o + 4\mathcal{B}$. The total transverse pressure is given as a function of ε and $\mathcal{E}$ in the three possible phases as

$$p(\varepsilon, \mathcal{E}) = \begin{cases} a_h T^4 = \frac{1}{3}\varepsilon & T < T_c \; ; \varepsilon < \varepsilon_H, \\ a_h T_c^4 = \frac{1}{3}\varepsilon_H(\mathcal{E}) & T = T_c \; ; \varepsilon_H < \varepsilon < \varepsilon_P, \quad 6.6 \\ a_q T^4 + \frac{1}{2}\mathcal{E}^2 - \mathcal{B} = \frac{1}{3}(\varepsilon - (4\mathcal{B} - \mathcal{E}^2)) & T > T_c \; ; \varepsilon_P < \varepsilon. \end{cases}$$

For a fixed value of $\mathcal{E}$, this 'extended bag equation of state' is qualitatively just like the ordinary bag equation of state ($\mathcal{E} = 0$ case) (see $[VI]$ Fig. 2). The latent heat associated with the transition at constant $\mathcal{E}$ is $\varepsilon_P - \varepsilon_H = 4\mathcal{B} - \mathcal{E}^2$. In the case $\frac{1}{2}\mathcal{E}^2 = \mathcal{B}$, the transition temperature and pressure vanish. The mixed state then consists of pure stable flux tubes (no matter is present),which occupy the fraction $r = \varepsilon/2\mathcal{B}$ of the total volume. In the general case the volume ratio is given by

$$r(\varepsilon, \mathcal{E}) = \begin{cases} 0 & T < T_c \; ; \varepsilon < \varepsilon_H, \\ (\varepsilon - \varepsilon_H)/(\varepsilon_P - \varepsilon_H) & T = T_c \; ; \varepsilon_H < \varepsilon < \varepsilon_P, \quad 6.7 \\ 1 & T > T_c \; ; \varepsilon_P < \varepsilon. \end{cases}$$

Plotting the boundary curves $r = 0$ and $r = 1$ on the $\mathcal{D} - s$ plane, we arrive at the 'phase diagram' of Fig. 8. Since $\mathcal{D}$ vanishes in the hadron phase ($r = 0$), the region corresponding to that phase on the $\mathcal{D} - s$ plane is just a line segment $(0, s_H^o = 4a_h T_{co}^3)$ on the s-axis.

6.2 Electrohydrodynamic equations of motion for the mixed state

In the previous section, an analogy between the mixed state and an ordinary dielectric medium was pointed out. Even though this analogy seems complete from the point of view of thermodynamics, it is not so, when the field equations are concerned. The reason for this is that, according to the spirit of bag model, we take the color-electric field to be *discontinuous* at the tube boundary . It is evident that the dynamic properties of the field consisting of a bunch of separate tubes are different from those of an ordinary continuous field. For example, a disturbance caused in the field in one tube can be mediated to the neighbouring tubes only by
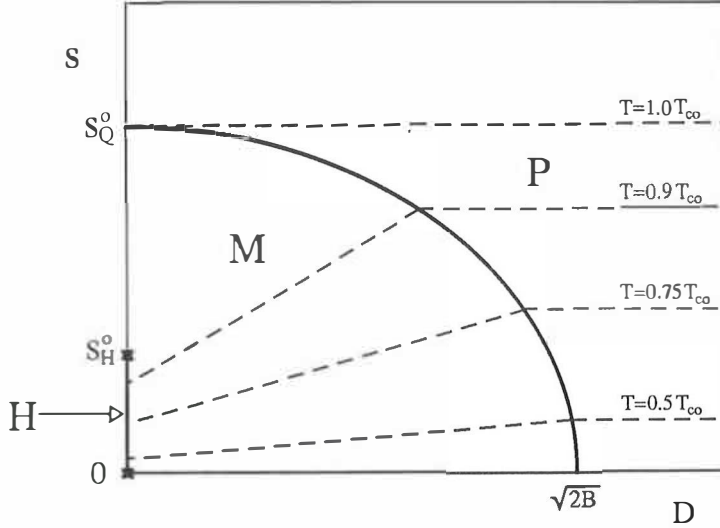
Fig. 8: The regions of hadron phase (H), mixed state (M) and plasma phase (P) on the $\mathcal{D} - s$ plane together with a few isotherms (dashed lines).

a pressure wave in the intermediary hadron gas. Secondly, the tube surfaces must always move with the transverse velocity of matter – a tube moving with respect to matter at uniform temperature would violate the conservation of energy and momentum at the surfaces. This implies, that the number of independent dynamic variables, and consequently, the number of independent equations of motion are reduced from that of the usual dielectric fluid. For the ordinary dielectric fluid, the Maxwell's equations are

$$\partial_\mu G^{\mu\nu} = J^\nu, \qquad\qquad 6.8$$

$$\partial_\mu \tilde{F}^{\mu\nu} = 0, \qquad\qquad 6.9$$

where the tensors $G^{\mu\nu}$ and $\tilde{F}^{\mu\nu}$ are related to the usual field tensor $F^{\mu\nu}$ by $G^{\mu\nu} u_\nu = \epsilon F^{\mu\nu} u_\nu$ and $\tilde{F}^{\mu\nu} = \frac{1}{2}\epsilon^{\mu\nu\alpha\beta} F_{\alpha\beta}$ [34]. These equations are also valid (with the dielectric constant $\epsilon = 1$) for the pure plasma case of ref. [29].

For an ordinary dielectric, these 'macroscopic' field equations are derived by averaging the 'microscopic' Maxwell's equations

$$\partial_\mu f^{\mu\nu} = j^\nu, \qquad\qquad 6.10$$

$$\partial_\mu \tilde{f}^{\mu\nu} = 0. \qquad\qquad 6.11$$

In doing so the continuity of the atomic scale field $f^{\mu\nu}$ and current j^ν is an essential assumption [34]. In the mixed state we assume that the eqs. $6.10 - 11$ are both valid in the interior of the tubes. However, if the color-electric field is parallel to the tube surface, the equation 6.10 is valid everywhere in spite of the discontinuity and can be averaged. Instead, the eq. 6.11 is not valid at the surface. Thus, we are only able to derive one averaged tensor equation, which is analogous and − with $G^{\mu\nu}$ and J^ν defined as averages of $f^{\mu\nu}$ and j^μ − formally identical with equation 6.8.

Another set of equations for the electrohydrodynamic flow of the mixed state is provided by the energy-momentum conservation law

$$\partial_\mu T^{\mu\nu} = 0, \qquad\qquad 6.12$$

where $T^{\mu\nu}$ is the total averaged energy-momentum tensor.

For cylindrically symmetric and boost invariant expansion of mixed state, there are three independent variables, which can be taken to be the transverse flow rapidity α, the entropy density s, and the field strenght $\mathcal{D}$. The latter two quantities are defined in the comoving frame of matter. Correspondingly, the equations 6.8 and 6.12 give three independent equations

$$T[\partial_\tau(s\,\mathrm{ch}\alpha) + \partial_\rho(s\,\mathrm{sh}\alpha) + \frac{s\,\mathrm{ch}\alpha}{\tau} + \frac{s\,\mathrm{sh}\alpha}{\rho}] = \mathcal{E}\mathcal{J} \qquad\qquad 6.13$$

$$s[\partial_\tau(T\mathrm{sh}\alpha) + \partial_\rho(T\mathrm{ch}\alpha)] + \mathcal{D}[\partial_\tau(\mathcal{E}\mathrm{sh}\alpha) + \partial_\rho(\mathcal{E}\mathrm{ch}\alpha) + \frac{\mathcal{E}\mathrm{sh}\alpha}{\tau}] = 0 \qquad 6.14$$

$$\partial_\tau(\mathcal{D}\mathrm{ch}\alpha) + \partial_\rho(\mathcal{D}\mathrm{sh}\alpha) + \frac{\mathcal{D}\mathrm{sh}\alpha}{\rho} = -\mathcal{J}, \qquad\qquad 6.15$$

where $\mathcal{J} = \kappa \mathcal{D} \sqrt{\mathcal{E}}$ is the magnitude of the polarization current arising from the particle production according to the Schwinger mechanism. Here, κ is a dimensionless constant, which depends on the boson and fermion coupling constants (see [29] eqs. 3.5 and 2.30).

6.3 One-dimensional expansion

In order to study the basic properties of the electrohydrodynamic evolution and the hadronization, controlled by the extended bag equation of state and the effective dielectric constant, we have solved the equations of motion neglecting the transverse expansion; i.e. by setting $\alpha \equiv 0$. The thermodynamic and field variables then depend only on τ and the eqs. $6.13 - 15$ reduce to two independent equations for entropy s and field $\mathcal{D}$,

$$ds/d\tau = -(s/\tau) - (\mathcal{E}\mathcal{J}/T),$$
$$dD/d\tau = -\mathcal{J},$$

6.16

which are valid for all three phases. In hadron phase, the latter equation is trivial and the upper one gives the usual Bjorken scaling solution $s\tau =$ constant. In the plasma phase $\mathcal{D} = \mathcal{E}$, the two equations decouple and can be solved analytically (refs. [29] and [V] Appendix). In the mixed state, the equations remain coupled through the equation $\mathcal{D} = r(s, \mathcal{E})\mathcal{E}$ and a numeric solution is needed. The initial condition is specified by setting the initial energy of the field in terms of bag constant as $\frac{1}{2}\mathcal{D}_o\mathcal{E}_o = \chi\mathcal{B}$.

In Fig. 9 the overall evolution is illustrated by representing the paths of the system on $\mathcal{D} - s$ plane for various values of χ.

If $\chi < 1$, the system is initially at the $\mathcal{D}$-axis point $\chi\sqrt{2\mathcal{B}}$ and consists of a bunch of stable flux tubes with a field strenght $\mathcal{E}_o = \sqrt{2\mathcal{B}}$ occupying a fraction χ of the total volume. If $\chi > 1$, the system is initially a giant flux tube corresponding to a point $\sqrt{\chi 2\mathcal{B}}$ on the $\mathcal{D}$-axis . The field is first rapidly converted into plasma particles resulting in increasing entropy and decreasing field strength. When the particle source (field) gets weaker, the entropy density starts to decrease due to the
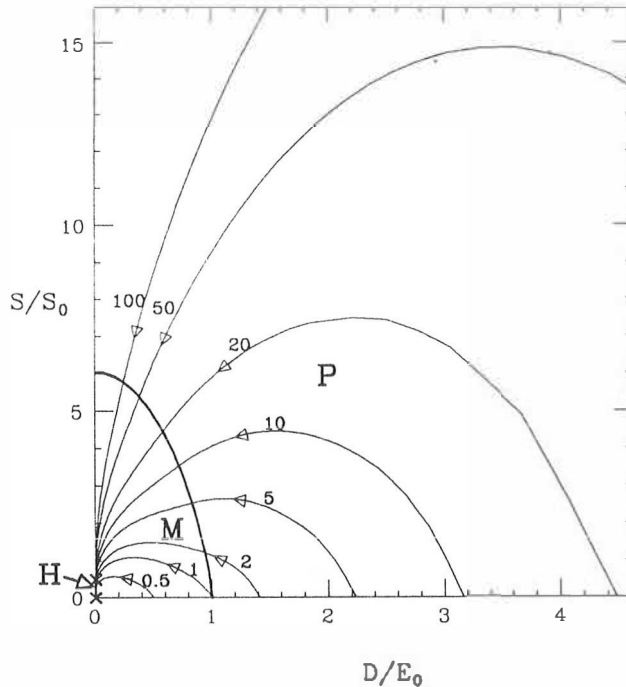
Fig. 9: The dynamic paths of the system on $\mathcal{D} - s$ plane in the one-dimensional scaling expansion for various values of the initial energy of the field $\frac{1}{2}\mathcal{E}_o\mathcal{D}_o = \chi\mathcal{B}$, $\chi = 0.5, ..., 100$. The units are given by $E_o = \sqrt{2\mathcal{B}}$ and $s_o = \mathcal{B}^{3/4}$.

longitudinal expansion. The system enters the mixed state, begins to hadronize and finally approaches the pure hadron phase at $\mathcal{D} = r = 0$. The hadronization process is illustrated in Fig. 10, in which the volume fraction r (the effective dielectric constant) is plotted as a function of time.

The time evolution of the temperature is shown in Fig. 11 for the cases $\chi = 1$ and $\chi = 20$ (solid lines) and compared with the ordinary Bjorken scaling solutions (dash-dotted lines) and, for the case $\chi = 20$, with the pure plasma ($\mathcal{B} = 0$) solution of ref. [29] (dashed line).

The Bjorken scaling solutions have been determined by requiring the (constant) total entropy dS/dy (or τs) of these solutions to be the same as the final entropy in the present numeric solutions. The $\chi = 20$ curve first follows the pure plasma solution during the particle production in the plasma phase. The initial field
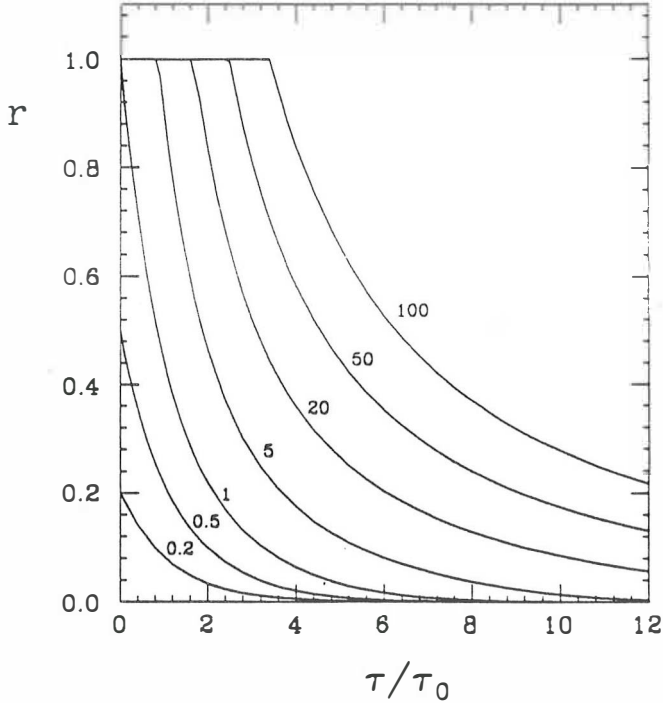
Fig. 10: The relative volume occupied by plasma $r = \Delta V_p(x)/\Delta V(x)$ (= the effective dielectric constant $\mathcal{D}/\mathcal{E}$) as a function of time. The proper time units are given by $\tau_o = 1/\kappa(2B)^{1/4}$. The curve labeling is as in Fig. 9.

decays rapidly and essentially just sets the 'initial temperature' for the subsequent ordinary scaling expansion. The major part of the particle production takes place in the plasma phase. The system undergoes sharp transitions first to the constant-temperature ($\sim T_{co}$) mixed state and finally to the hadron phase in which the temperature is proportional to $(1/\tau)^{1/3}$. Note especially the clear transition at the point marked τ_H^{20}, which coincides with the mixed to hadron transition of the corresponding ordinary scaling solution. For the higher values of χ the transition to the corresponding scaling solution is even more rapid and complete. We thus see that if the initial energy of the field is high compared to the bag constant, the present scenario is essentially reduced to setting the initial condition for the subsequent ordinary hydrodynamic expansion using the bag equation of state.

For the lower values of χ the field remains relatively important in the mixed
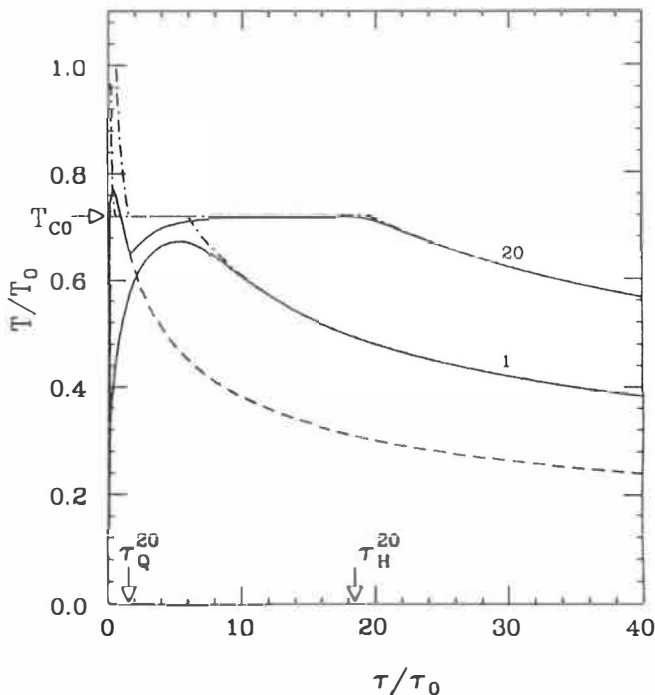
Fig. 11: The time evolution of the temperature for scaling solution using the extended bag equation of state for the cases $\chi = 1$ and $\chi = 20$ (solid lines). The dash-dotted lines are the corresponding ordinary scaling solutions with bag equation of state (same final entropy) . The points τ_Q^{20} and τ_H^{20} give the transition times from plasma to mixed phase and from mixed to hadron phase, respectively, for the ordinary scaling solution corresponding to $\chi = 20$. The dashed line is the pure plasma ($\mathcal{B} = 0$) solution with the same initial field energy as in the case $\chi = 20$ [28]. T_{co} is the transition temperature at zero field in the units $T_o = \mathcal{B}^{1/4}$. The time unit is as in Fig. 10.

state, where a large fraction of the particles are produced. The temperature $T = T_c(\mathcal{E})$ does not remain constant in the mixed state, but varies with the field $\mathcal{E}$ according to eq. 6.1. The smooth asymptotic transition to hadron phase occurs at temperatures well below T_{co} as shown by the $\chi = 1$ curve in Fig. 11. Thus, if the initial field energy is not too large, the evolution through the mixed state and

the transition to hadron phase are qualitatively different from those of the usual scaling hydrodynamics.

It will be interesting to study whether the extended bag equation of state leads to a mixed-hadron rarefaction shock in the case of a free transverse expansion in analogy to the ordinary bag equation of state [17]. How is the transverse expansion affected by the modifications in this transition or by the fact that due to the field contribution, pressure gradients can be present in the mixed state. It will also be interesting to study the relation between the transverse momentum and the total entropy and to see, whether the approximate scaling of $\langle p_T \rangle$ as a function of $(1/A)dN/dy$ (or perhaps rather as a function of $(1/A)^{5/6}dN/dy$), as predicted by the ordinary hydrodynamics $[II]$, is preserved in the present model.

7. Three-dimensional hydrodynamics of O+Pb collisions

The numeric calculations presented in refs. $[I - V]$ and reviewed in the previous sections consider the central region of a head-on collision of two identical heavy nuclei at energies $\sim 100 + 100$ GeV/nucleon, which may become available in the future at RHIC. At these energies, the simplifying assumptions of a boost invariant flow and a negligible baryon number density are expected to be justified in the central region. In the present CERN experiments the situation is more complicated both geometrically and dynamically. A realistic hydrodynamic calculation should probably deal with several interpenetrating fluids, and take into account their interactions, the non-vanishing baryon number and the finite and non-trivial longitudinal dimension [15, 16]. A step to that direction has been taken in ref. $[VI]$, where a 1+2 dimensional version of the SHASTA-FCT code is applied to find a numeric solution for the expansion of a finite cylinder of matter, which is assumed to be formed in a central $O + Pb$ collision at 200 MeV/nucleon. The Landau type initial condition is fixed using a simple geometrical picture of the collision: All the available energy is deposited evenly into a cylinder of radius R_O and lenght $2R_{Pb}/\gamma_{cm}$ – the 'hot tube' (Fig. 1(a)). The possible non-complete stopping of nuclear matter is simulated by using also an initial condition with a

non-zero velocity in the longitudinal direction. We note that the nucleons are still ignored; the phase transition at $T_c = 200\,MeV$ is simulated by the bag equation of state at zero chemical potential of baryons. A comparison to the case without a phase transition is made by using also the equation of state for ideal gas of massless pions, $p = (1/3)\varepsilon$. The pseudorapidity distribution of the transverse energy is calculated for massless pions, which decouple at a fixed temperature $T_{dec} = 140\,MeV$.

In Fig. 12, the hydrodynamic evolution of the hot tube is shown as contour plots of the comoving energy density ε and the transverse velocity v_r at fixed times for the case of vanishing initial velocity of the fluid.

For the energy density, only the contours $\varepsilon_{dec} = 0.05$ GeV/fm^3, $\varepsilon_H = 0.2$ GeV/fm^3 and $\varepsilon_Q = 3.8$ GeV/fm^3 are shown. In the CM frame the initial volume is a cylindrical disk of radius 2.8 fm and length 2.4 fm of which only one half is shown on the $r - z$ plane. The matter is initially in the plasma state at temperature $T_o \sim 260$ MeV and at rest. The region of pure plasma phase with $\epsilon > \epsilon_Q$ breaks rapidly into two ellipsoidal parts, which move apart in the z direction. The plasma is just disappearing in the figure with $t = 5$ fm. By contrast, due to its vanishing pressure gradient the bulky mixed phase with $\epsilon_H < \epsilon < \epsilon_Q$ survives through the entire evolution. This region is emptied slowly through the accelerating shock front on its outer boundary. The hadron phase with $\epsilon_{dec} < \epsilon < \epsilon_H$ is mostly a thin mantle around the mixed phase core. Shortly after the time $t = 15$ fm, the entire 'hydrodynamic' region with $\epsilon > \epsilon_{dec}$ is broken into two portions moving apart with velocities $v_z \sim \pm 0.4$ in the CM frame until they decouple entirely at $t \sim 30$ fm. During this long period of time the cigar shaped boundary between the mixed and the hadron phases effectively converts the flow into transverse direction leading to a very high total transverse energy. The breakup to two portions takes place because of the combined effect of the longitudinal rarefaction waves, which propagate in the plasma phase and are reflected at $z = 0$, and of the time dilation effect caused by the strong longitudinal flow.

In the absence of the phase transition, the flow is much simpler than in the previous case. The longitudinal and transverse rarefaction waves propagate freely to the
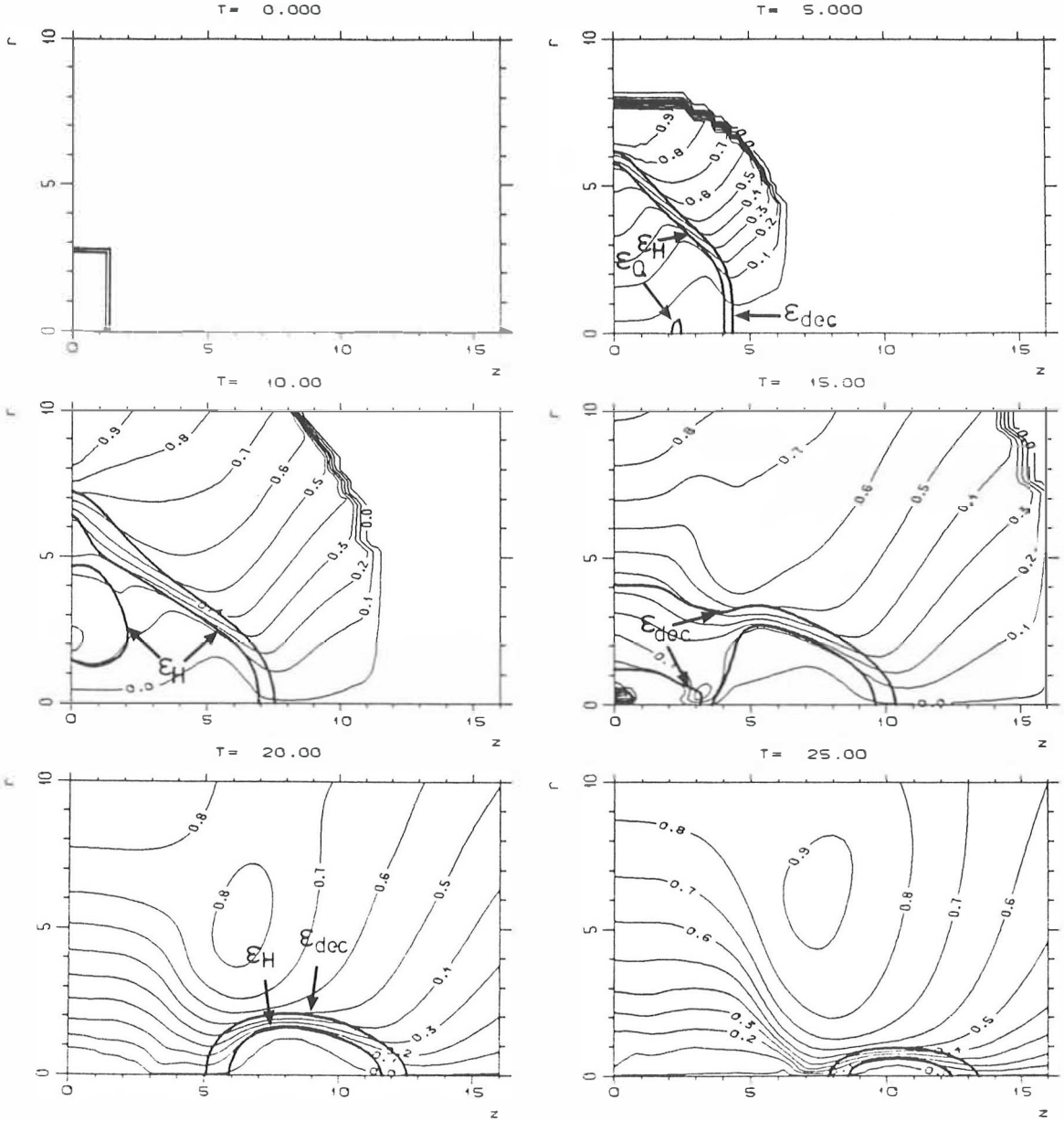
Fig. 12: The evolution of the hot tube given as contour curves for constant transverse velocity v_r (thin lines) and three constant energy density contours $\varepsilon_{dec} = 0.05$ GeV/fm^3, $\varepsilon_H = 0.2$ GeV/fm^3 and $\varepsilon_Q = 3.8$ GeV/fm^3 (heavy lines) at fixed times $t = 0, 5, ..., 25$ fm. The initial velocity $v_r^o = v_z^o = 0$, the initial temperature $T_o = 260$ MeV and the critical temperature $T_c = 200$ MeV.

interior of the system with the velocity of sound. Due to the initial shape of the hot tube, the flow is very strong in the longitudinal direction leading to a rapid expansion and to a lower transverse energy than in the presence of the phase transition. However, the average transverse energy per particle is higher than in the case with a phase transition because for a fixed total initial energy and volume, the total entropy is higher for the plasma than for the pion gas.

Due to the assumed complete thermalization of all the available energy, the calculated transverse energies tend to be high. For the case of vanishing initial velocity, the transverse energy in the pseudorapidity interval $-0.1 < \eta < 2.9$ was found to be 345 GeV and 260 GeV for the cases with and without phase transition, respectively. This is to be compared with the highest value of $\sim$ 200 GeV measured by the CERN NA34 group for the same pseudorapidity interval [10a]. By taking the longitudinal velocity of the fluid to be initially $v_z = \mathrm{th}(z/z_L)$, where $z_L = R_{Pb}/\gamma_{cm} = 1.2$ fm, the calculated transverse energies were reduced to values 270 GeV and 180 GeV for the cases with and without phase transition, respectively. Obviously, lower values of the transverse energy can be achieved also by assuming that only a fraction of the original kinetic energy of the colliding nuclei is thermalized.

The main purpose of this work was to test the numeric method based on the SHASTA-FCT algorithm to integrate the 1+2 dimensional hydrodynamic equations to be used later in the context of more involved models. In the present (over)simplified hydrodynamic scenario for O+Pb central collisions, the method proved effective and qualitatively reliable. The calculated distributions are sensitive to the initial conditions and to the equation of state and can possess a non-trivial structure due to the complicated collective effects.

8. Outlook

Since the discovery of the underlying quark structure of hadrons, many measurements have been proposed, and recently also performed, with the goal of verifying the existence of quark-gluon plasma in ultrarelativistic heavy ion collisions. The recent experiments at CERN and Brookhaven do not yet give a clear-cut answer to this question, but they do suggest that the nuclear collisions may provide a system, which is large enough for a meaningful search for collective effects – including the formation of the new phase of matter.

The Relativistic Heavy Ion Collider (RHIC), which is planned to be built at Brookhaven National Laboratory, would provide a considerably higher energy and a larger nuclear system, which at least from theoretical point of view would be less complicated than what is presently available. In this work I have presented a series of studies, which are based on the use of hydrodynamics to solve the evolution of matter produced in ultrarelativistic heavy ion collisions. Most of the calculations concern the energy range and the geometrical set-up which would be characteristic to RHIC. The numeric solution of hydrodynamic equations was used to extract several quantities, which could be used to signal the existence of various collective phenomena. A simple bag model equation of state was utilized to simulate qualitatively a first order phase transition between the hadronic matter and the quark-gluon plasma.

The categorical advantage of the present approach is its simplicity and feasibility. However, the system under study is complicated. The non-thermal phenomena, especially at the early and late stages of the evolution, may obscure the signals from thermal sources. For example, the lepton pairs and strange particles can be produced by several competing mechanisms, which may hide the proposed signals of a quark-gluon plasma. More knowledge of these phenomena are needed in order to find exclusive tests of plasma production.

References:

[I]   -H. von Gersdorff, L. McLerran, M. Kataja, P. V. Ruuskanen, Phys. Rev. D**34**, 794 (1986)

[II] -M. Kataja, P. V. Ruuskanen, L. McLerran and H. von Gersdorff, Phys. Rev. D**34**, 2755 (1986).

[III] -K. Kajantie, M. Kataja, L. McLerran and P. V. Ruuskanen, Phys. Rev. D**34**, 811 (1986).

[IV] - K. Kajantie, M. Kataja, P. V. Ruuskanen, Phys. Lett. B**179**, 153 (1986).

[V] -M. Kataja, T. Matsui, MIT preprint CTP# 1693 (1989), Submitted to Annals of Physics.

[VI] -M. Kataja, Z. Phys. C**38**, 419 (1988).

——

[1] -M. Gell-Mann, Phys. Lett. **8**, 214 (1964).
     -M. Gell-Mann, Y. Ne'eman, *The Eightfold Way*, W. A. Benjamin, N.Y. 1964.

[2] For a general rewiev, see for example:
     -J. Cleymans, R. U. Gavai, E. Suhonen, Phys. Rep. **130**, 217 (1986).
     -Proceedings of the Sixth International Conference on Ultra-Relativistic Nucleus-Nucleus Collisions (Quark Matter '87), edited by H. Satz, H. J. Specht, R. Stock, Z. Phys. C**38** Nr. 1/2, (1988).
     -Proceedings of the Seventh International Conference on Ultra-Relativistic Nucleus-Nucleus Collisions (Quark Matter '88), edited by S. Nagamiya, G. Baym, P. Braun-Munzinger, Nucl. Phys. A in press.

[3] -A. Polyakov, Phys. Lett. B**42**, 477 (1978).
     -L. Susskind, Phys. Rev. D**20**, 2610 (1979).
     -B. Svetitsky, Nucl. Phys. A**461**, 71c (1987);
     -F. Karsch, Z. Phys. C**38**, 147 (1988).

[4] -J. Engels, F. Karsch, I. Montvay, H. Satz, Phys. Lett. B**101**, 89 (1981).
     -L. D. McLerran, B. Svetitsky, Phys. Lett. B**98**, 195 (1981).

-K. Kajantie, C. Montonen, E. Pietarinen, Z. Phys. C9, 253 (1981).

-J. Kuti, J. Polónyi, K. Szlachányi, Phys. Lett. B98, 199 (1981).

[5] -K.Olive, Nucl. Phys. B190, 483 (1981).

-E. Suhonen, Phys. Lett. B119, 81 (1982).

-D. Schramm, K. Olive, Nucl. Phys. A418, 289 (1984).

-T. DeGrand, K. Kajantie, Phys. Lett. B147, 273 (1984).

[6] -E. Witten, Phys. Rev. D30, 272 (1984).

-L. F. Abbott in *Proceedings of Quark Matter '84*, ed. K. Kajantie, Springer Verlag, 1985.

[7] -D. Ivanenko, D. F. Kurgelaidze, Lett. Nuovo Cim. 2, 13 (1969).

-N. Itoh: Progr. Theor. Phys. 44, 291 (1970).

[8] -E. V. Shuryak, Phys. Lett. B78, 150 (1978),

-R. Anishetty, P. Koehler, L. McLerran, Phys. Rev. D22, 2793 (1980),

-K. Kajantie, L. McLerran, Phys. Lett. B119, 203 (1982).

[9] -J. D. Bjorken, Phys. Rev. D27, 140 (1983)

[10] CERN-SPS experiments:

10a. NA34 (HELIOS):

-T. Åkersson, et. al. Z. Phys. C38, 383 (1988); Phys. Lett. B197, 295 (1988); Z. Phys. C38, 15 (1988).

10b. NA35:

-A. Bamberger, et. al. Phys. Lett. B184, 271 (1987); Phys. Lett. B203, 320 (1988); Phys. Lett. B205, 583 (1988); Z. Phys. C38, 19, 79, 89, 125 (1988).

10c. NA36:

-P. D. Barnes, et. al. Phys. Lett. B206, 146 (1988).

10d. NA38:

-M. C. Abreu, et. al. Z. Phys. C38, 117, 129 (1988);

10e. WA80:

-R. Albrecht, et. al. Phys. Lett. B199, 297 (1987); Phys. Lett. B201, 390

(1988); Phys. Lett. B**202**, 596 (1988); Z. Phys. C**38** 3, 51, 109 (1988).

    10f. EMU-01:

        -M. I. Adamovich, et. al. Phys. Lett. B**201**, 397 (1988).

[11] BNL-AGS Experiments:

    11a. E802:

        -T. Abbott, et. al. Phys. Lett. B**197**, 285 (1987); Z. Phys. C**38**, 35 (1988).

    11b. E814:

        -B. Bassalleck, et. al. Z. Phys. C**38**, 45 (1988).

[12] -S. S. Padula, M. Gyulassy, LBL-26076 Preprint (1988). To be published in Proc. of QM'88, Nucl. Phys. A, ed. G. A. Baym, et. al.
-M. Gyulassy, S. S. Padula, LBL-26077 Preprint (1988).

[13] -S. Pratt, Phys. Rev. D**33**, 1314 (1986).

[14] -J. Stachel, P. Braun-Munzinger, Phys. Lett. B**216**, 1 (1989).

[15] -T. Rentzsch, G. Graebner, J. A. Maruhn, H. Stöcker, W. Greiner, Z. Phys. C**38**, 237 (1988).

[16] -H. W. Barz, B. Kämpfer, L. P. Csernai, B. Lukács, Nucl. Phys. A**465**, 743 (1987).

[17] -P. Danielewicz, P. V. Ruuskanen, Phys. Rev. D**35**, 344 (1987).
-B. L. Friman, K. Kajantie, P. V. Ruuskanen, Nucl. Phys. B**266**, 468 (1986).

[18] -J. P. Blaizot, J. Y. Ollitrault, Phys. Rev. D**36**, 916 (1987).

[19] -J. P. Boris, D. L. Book, J. Comp. Phys. **11**, 38 (1973);
-D. L. Book, J. P. Boris, K. Hain, J. Comp. Phys. **18**, 248 (1975);
-J. P. Boris, D. L. Book, J. Comp. Phys. **20**, 397 (1976).

[20] -S. T. Zalesak, J. Comp. Phys. **31**, 335 (1979).

[21] - E. Cooper, G. Frye, Phys. Rev. D**10**, 186 (1974).
- E. Cooper, G. Frye, E. Schonberg, Phys. Rev. D**11**, 192 (1975).

[22] -P. V. Ruuskanen, Z. Phys. C**38**, 219 (1988).

[23] -P. Koch, B. Müller, J. Rafelski, Phys. Rep. **142** (1986).

[24] -B. Müller, *The Physics of the Quark-Gluon Plasma*, Lecture Notes in Physics **225**, Springer Verlag, Heidelberg, (1985).

[25] -J. Rafelski, B. Müller, Phys. Rev. Lett. **48**, 1066 (1982).
-T. Matsui, B. Svetitsky, L. D. McLerran, Phys. Rev. D**34**, 783 (1986).

[26] -J. Kapusta, A. Mekjian, Phys. Rev. D **33**, 1304 (1986).

[27] -H. W. Barz, B. L. Friman, J. Knoll, H. Schulz, Nucl. Phys. A**484**, 661 (1988).

[28] -H. Ehtamo, J. Lindfors, L. McLerran, Z. Phys. C**97**, 341 (1983).
-K. Kajantie, T. Matsui, Phys. Lett. B**164**, 373 (1985);
-A. K. Kerman, T. Matsui, B. Svetitsky, Phys. Rev. Lett. **56**, 219 (1986);
-A. Białas and W. Czyż, Phys. Rev. D**31**,198 (1985);
-A. Białas, W. Czyż, A. Dyrek, W Florkowski, Nucl. Phys. B**296**, 611 (1988).

[29] -G. Gatoff, A. K. Kerman, T. Matsui, Phys. Rev. D**36**, 114 (1987).

[30] -T. S. Biro, H. B. Nielsen, and J. Knoll, Nucl. Phys. B**245**, 449 (1984);
-J. Knoll, Z. Phys. C**38**,187 (1988).

[31] -J. Schwinger, Phys. Rep. **82**, 664 (1951).
-N. K. Glendenning, T. Matsui, Phys. Rev. D**28**, 2890 (1983).

[32] -J. Kogut, L. Susskind, Phys. Rev. D**9**, 3501 (1974).
-T. D. Lee,Phys. Rev. D**19**, 1802 (1979).

[33] -H. Lehman, T. T. Wu, Nucl. Phys. B**237**, 205 (1984).
-H. Lehman, Nucl. Phys. B**271**, 166 (1986).

[34] -L. D. Landau, E. M. Lifshitz, L. P. Pitaevskiĭ: *Electrodynamics of Continuous Media*, Pergamon Press, Oxford (1984).